Hexagon-on-cube versus cube-on-cube epitaxy: The case of ZnSe(111) on $SrTiO_3$(001)

B. Rache Salles, K. Kunc, M. Eddrief, V. H. Etgens, F. Finocchi, and F. Vidal
Institut des Nanosciences de Paris (INSP), Université Pierre et Marie Curie-Paris 6, CNRS UMR 7588, Campus de Boucicaut, 140 rue de Lourmel, 75015 Paris, France

(Received 3 February 2009; revised manuscript received 10 March 2009; published 17 April 2009)

The structure of ZnSe epilayers grown by molecular-beam epitaxy on $SrTiO_3$(001) substrates has been studied using electron diffraction, x-ray diffraction, and electron microscopy. ZnSe, like certain other zinc-blende semiconductors, grows epitaxially along the [111] direction, contrary to what is expected from considerations on lattice registry and mismatch. First-principles calculations based on density-functional theory show that this peculiar epitaxy results from the subtle balance between strain and interface bonding during the growth of the first layer.

DOI: 10.1103/PhysRevB.79.155312 PACS number(s): 68.55.−a, 71.15.Nc, 81.15.Hi

I. INTRODUCTION

Oxide materials exhibit a wide spectrum of physical properties such as high-temperature superconductivity,[1] colossal magnetoresistance,[2] metal-insulator transitions,[3] etc. In recent years, there has been an increasing effort of research on thin films and heterostructures that are made of functional oxides.[4] Combining such compounds with semiconductors (SC) is an appealing perspective with relevant applications in electronics. Among functional oxides, many interesting systems crystallize in the cubic perovskite structure. The prototype of this class of oxides is strontium titanate, $SrTiO_3$ (STO). Successful cube-on-cube (CoC) epitaxial growth of STO on GaAs(001) has been recently reported.[5] However, despite moderate lattice mismatch after in-plane 45° rotation, the *reverse* epitaxy of zinc-blende semiconductors (ZB-SC) on $SrTiO_3$(001) is totally different. Results reported so far show that some ZB-SC [GaAs (Ref. 6) and InP (Ref. 7)] grow along the [111] direction. Considering the obvious difference between the hexagonal and square registries, this particular orientation remains surprising and, so far, no satisfactory explanation has been proposed for this counterintuitive configuration. Deeper understanding of the origin of this epitaxy is desirable to progress in the field of SC/oxide heterostructural growth. Most of the studies reported so far dealt with III-V ZB-SC. II-VI ZB-SC have a higher ionic character than III-V ZB-SC, which may influence the growth. In this paper, we examine the growth of II-VI ZB-SC ZnSe epilayers on $SrTiO_3$(001). We evidence the hexagon-on-cube (HoC) growth of the ZnSe overlayers by reflection high energy electron diffraction (RHEED), x-ray diffraction, and transmission electron microscopy (TEM). Through first-principles calculations, we propose an explanation of the peculiar interface formation, which is based on the structures and the energetics of the first ZnSe epilayers.

Before reporting our results on the ZnSe/$SrTiO_3$(001) system, we would like to point out that hexagon-on-cube epitaxy has been observed in other systems, such as InN on 3C-SiC(001).[8] However, in that study, the InN overlayer has a hexagonal wurtzite structure which is the same symmetry as in the bulk InN. The hexagon-on-cube epitaxy is thus less surprising than in the case we report here.

II. EXPERIMENTS

ZnSe epilayers were grown by solid source molecular-beam epitaxy (MBE) on (001)-oriented $SrTiO_3$ substrates (SurfaceNet GmbH). Prior to growth, the STO substrates were heated at 750 °C under the atomic oxygen flux delivered by a plasma source to obtain a clean TiO_2-terminated (1×1) surface, as shown by the RHEED diagram in Fig. 1(a). After this procedure, the samples were transferred under ultrahigh vacuum in a II-VI MBE chamber equipped with Zn and Se cells. MBE deposition was then carried out at various growth temperatures (T_g) in the 180–280 °C range. We exposed the surface to a Zn flux and then kept the Se/Zn flux ratio at two, which has been optimized for the growth of pseudomorphic ZnSe/GaAs(001) epilayers.[9] The growth rate was 5 Å min^{-1} as determined *a posteriori* by TEM and x-ray reflectivity. In what follows we focus on the results obtained for $T_g=220$ °C. Growth at other temperatures yielded essentially the same results with a slight degradation of the structural quality.

Considering the lattice parameter of both materials (2.6% misfit) and their cubic structures, one expects that the ZnSe would adopt the CoC epitaxy, with the following epitaxial relationship: $(001)_{ZnSe}\|(001)_{STO}$, $[100]_{ZnSe}\|[110]_{STO}$. Surprisingly, this is not observed. The RHEED diagrams [quasi-two-dimensional (2D) at the beginning of the growth and three-dimensional (3D) after ~10 min] are shown in Fig. 1(a). They are obtained for an azimuthal angle corresponding to the [100] direction of STO and were found to repeat identically with an azimuthal period of 30°. All the spots appearing in the 3D diagram of Fig. 1(a) could be indexed, as shown in Fig. 1(b), revealing a (111)-oriented ZnSe epilayer with four types of epitaxial domains.[10] The θ-2θ scan depicted in Fig. 1(d) confirms the (111) orientation and the ϕ scan (inset) shows the existence of four types of rotational domains. The epitaxial relationship can be summarized as follows: $(111)_{ZnSe}\|(001)_{STO}$ and $[1\bar{1}0]_{ZnSe}\|[100]_{STO}$ or equivalent directions.[11] A high-resolution TEM image of such a domain in the interfacial region is shown in Fig. 1(e). From the spacing of atomic rows, we determine a lattice mismatch of $2.7\pm0.4\%$, which agrees with the 2.6% mismatch that is expected from the respective bulk lattice parameters. The ZnSe supported film relaxes to its own bulk

 ©2009 The American Physical Society

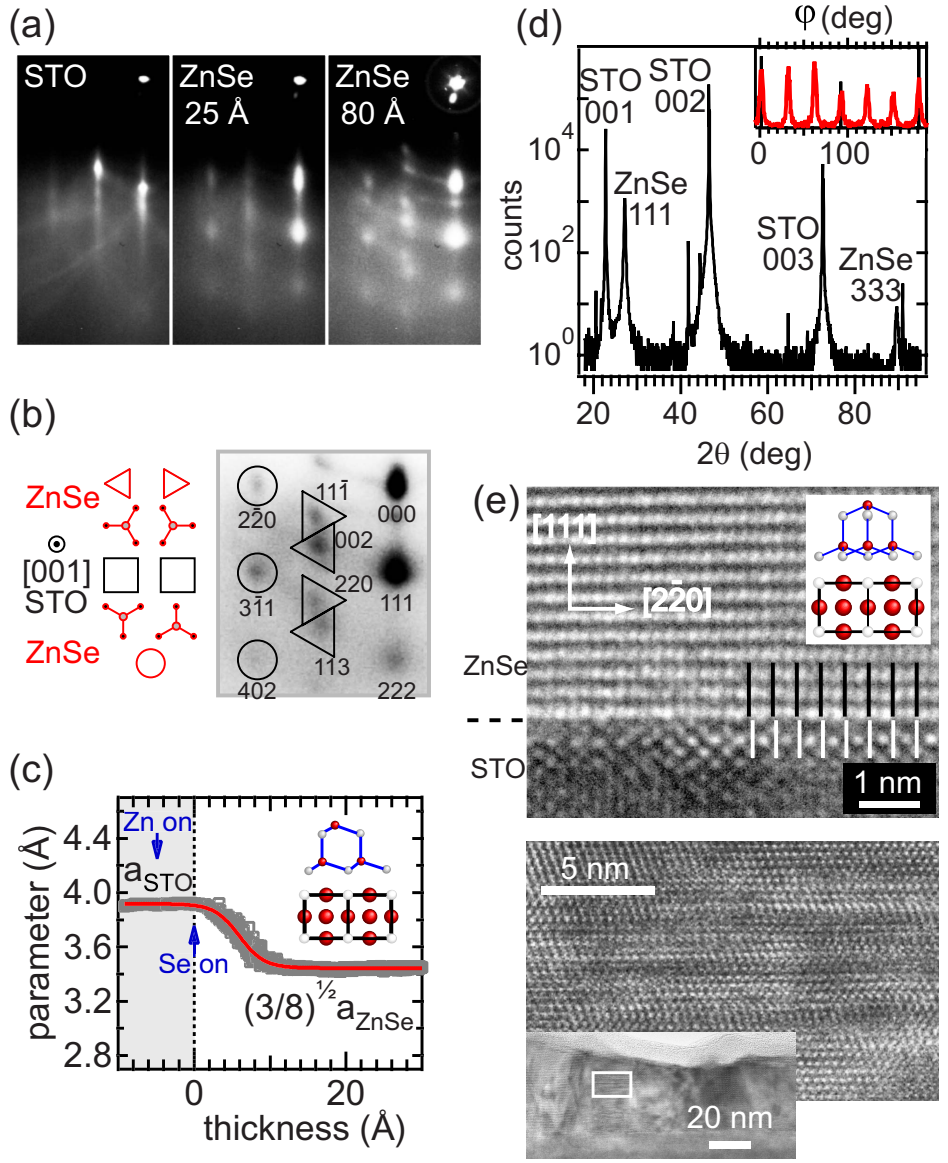

FIG. 1. (Color online) (a) RHEED diagram of the (1×1) $SrTiO_3$ surface along [100] (electron beam along [010]) after annealing under atomic oxygen, RHEED of the ZnSe layer, same azimuth, after 5 and 16 min of growth. Only half diagrams are shown. (b) Scheme of ZnSe in plane orientation with respect to the TiO_2-terminated (1×1) $SrTiO_3$ surface unit cell. Triangles and circles indicate the corresponding indexed spots in the RHEED diagram with inverted contrast. (c) Relaxation of lattice parameter along $[11\bar{2}]$ of ZnSe ($a_{ZnSe}\times\sqrt{3}/2\sqrt{2}$ =3.47 Å). (d) θ-2θ scan of a 40 nm ZnSe layer grown on $SrTiO_3$. Inset: Thick red (dark gray) line: ϕ scan of ZnSe (220) showing a 30° periodicity, along with $SrTiO_3$ (110) (thin black line). (e) Higher part: High resolution TEM image of the ZnSe/$SrTiO_3$ interface. Zone axis: $[11\bar{2}]_{ZnSe}$. Lower part: TEM image of a region with stacking faults, the inset shows a view of the film with the zoom region delimited by a white rectangle.

lattice constant, as substantiated by the parameters evolution along $[11\bar{2}]_{ZnSe}$. This is depicted in Fig. 1(c) where the initially strained film is seen relaxing in the early stage of growth, within the first 10 Å (equivalent film thickness). The picture that emerges from these measurements is the growth of a strained ZnSe film followed by relaxation, most probably ensured by the formation of misfit dislocation at the interface.

III. CALCULATIONS

In order to get insights into the experimental data, we performed first-principles calculations by using the density-functional theory (DFT) within the local-density approximation. All the way through, we examine, in parallel, the growth of ZnSe overlayers along the [111] and [001] directions. The calculations have been performed using the VASP code[12] within the projector augmented wave (PAW) formalism.[13,14] The PAW potentials were constructed by Kresse and co-workers;[12] for oxygen we are using the one denoted as O_s in Ref. 12. The energy cutoff on plane waves was set at 283 eV, and the k-point sampling of the reciprocal space was performed on $2\times2\times2$ and $4\times4\times2$ homogeneous meshes of the Monkhorst-Pack type.[15] From preliminary tests on the ZnSe and $SrTiO_3$ cubic crystals, we ob-

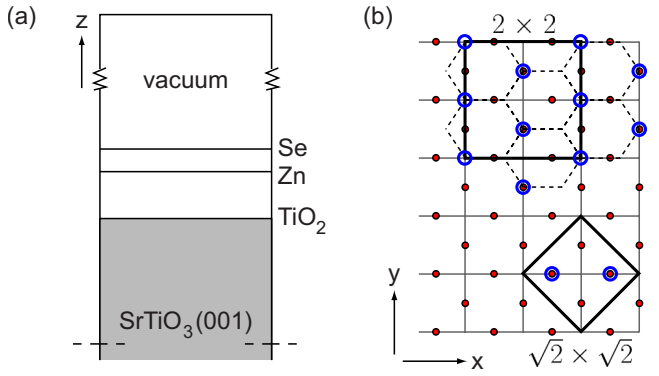

FIG. 2. (Color online) Schematic representation of the interface atomic models studied by the *ab initio* calculations in this work. (a) Side view: periodic-supercell geometry. A substrate consisting of $SrTiO_3(001)$ planes (thickness of $2a_{STO}$), one layer of ZnSe(111) [or, alternatively, ZnSe(001); not shown], and vacuum. Only half of the supercell is given, the "lower" part is constructed symmetrically. (b) Top view: relative position of the substrate and overlayers. Red (dark gray) dots=oxygen; circles=zinc. The small squares correspond to the TiO_2 surface of $SrTiO_3(001)$, with Ti atoms (not shown) situated in the middle of every square. The hexagons representing the Zn plane of ZnSe(111) are deformed by 12.5% along x and by −2.6% along y. The STO(2×2) translational unit is highlighted. In the lower right-hand corner we show the $\sqrt{2}\times\sqrt{2}$ translational unit used in the alternative calculations with the ZnSe(001) overlayers. Here the Zn-Zn distances are deformed by −2.6% so as to match the TiO_2 registry. Directions x and y are [100] and [010] of STO; they correspond to $[11\bar{2}]$ and $[1\bar{1}0]$ of ZnSe in the upper picture, and to ZnSe$[1\bar{1}0]$ and [110] in the lower one.

tained the theoretical equilibrium lattice constants: $a_{SrTiO_3}=3.868$ Å and $a_{ZnSe}=5.577$ Å, to be compared with experimental values, 3.905 and 5.667 Å, respectively. They are employed in all the calculations on the $ZnSe/SrTiO_3(001)$ model interfaces. In all configurations, we relax the atomic positions until the forces become smaller than 5 meV/Å and the energy reaches the nearest local minimum.

We focus on the initial stages of the growth, which are decisive for the formation of the ZnSe overlayers. We perform calculations on single and double ZnSe layers (two or four atomic planes, respectively) on the $SrTiO_3$ substrate. As shown schematically in Fig. 2(a), abrupt interfaces are assumed throughout, consistently with the TEM images in Fig. 1 and previous results for several III-V semiconductors on $SrTiO_3$.[6] The top view of the substrate—the (001) plane of $SrTiO_3$—and the relative positions of the overlayers are shown in Fig. 2(b). In order to discuss the relative stability of the configurations, we rely mainly on the *adlayer formation energy* E_{form}^{ZnSe}, which is the energy gained in passing from the clean relaxed $SrTiO_3(001)$ surface plus Se and Zn atoms to the final configuration of ZnSe overlayer(s) on $SrTiO_3(001)$. Therefore, E_{form}^{ZnSe} can be seen as a measure of the stability of the ZnSe adlayers deposited through MBE, whenever thermodynamic equilibrium is attained.

With regards to the stability of the interface between ZnSe and $SrTiO_3$, one has to consider the polar character of such a heterojunction since both (001) and (111) orientations of ZnSe are polar. Therefore, for increasing thickness of the ZnSe epilayer, the whole system must be polar compensated[16] or, equivalently, fulfill the electron counting rule.[16,17] This poses practical restrictions on the composition of the Zn and Se layers at the interfaces with $SrTiO_3$ and with vacuum. However, as recently pointed out,[16,18] ultrathin films grown along a polar direction can also sustain a net polarization up to a threshold thickness. Therefore, for ZnSe overlayers on $SrTiO_3(001)$, we allow both polar-compensated and uncompensated layer sequences as candidates for metastable configurations, as reported in Table I.

TABLE I. Formation energies of ZnSe overlayers on $SrTiO_3(001)$ (in eV per ZnSe formula unit), as a function of the number of atomic planes n and the growth direction. A larger E_{form} corresponds to more stable structure. The schematic layer sequence of the most stable configurations is also indicated, starting from the contact with the substrate. For $n=2$ uncompensated sequences are favored while for $n=4$ (and beyond) the most stable structures are polar compensated.

Orientation	n	Sequence of at. planes	E_{form}^{ZnSe}
[001]	2	Zn/Se	7.13
[111]	2	Zn/Se	7.18
[001]	4	$Zn_{0.5}/Se/Zn/Se/Zn_{0.5}$	7.13
[111]	4	$Zn_{0.75}/Se/Zn/Se/Zn_{0.25}$	7.01

In order to identify the most stable type of contact at the interface, a full thermodynamic analysis in terms of the chemical potentials would be needed (see Ref. 19 and references therein). However, we restrict ourselves to the case $N_{Zn}=N_{Se}$, which should be representative of the experimental conditions.

First, we examine hypothetical ZnSe(001) on STO(001) structures by choosing a nonelementary translational unit STO ($\sqrt{2}\times\sqrt{2}$) in order to allow for polarity compensation. The epitaxial relationships are shown in Fig. 2(b): the squared unit cell of ZnSe is turned by 45° and the ZnSe lattice deformation required for pseudomorphic growth is merely −2.6%. We also vary the nature of the contacts at the interface and shift the origin of the ZnSe planar unit cell with respect to the substrate. By comparing their total energies, most of the 16 inequivalent configurations can be discarded, and the lowest-energy structures corresponding to different contacts at the interface are found out. The most stable configuration for the ZnSe (001) single layer ($n=2$) shows Zn-Se zigzag chains along the [110] direction; Zn atoms are bound to O and Se atoms are on top of Ti [Fig. 3(a)]. This is fully consistent with previous findings on other compound semiconductors grown on $SrTiO_3(001)$ (Ref. 19) and is chemically sound, as the interface Zn atoms are easily oxidized. However, the Zn-Se chains are loosely bound to each other. Although the interlayer distance between Zn and Se planes is considerably reduced, the Zn-Se bonds are stretched. Both the interaction with the substrate and the reduction in the dipole moment are responsible for such a behavior. The formation energy turns out to be 7.13 eV/ZnSe unit.

Second, we consider eight inequivalent candidates to the [111]-oriented ZnSe layer on STO(001), which were con-

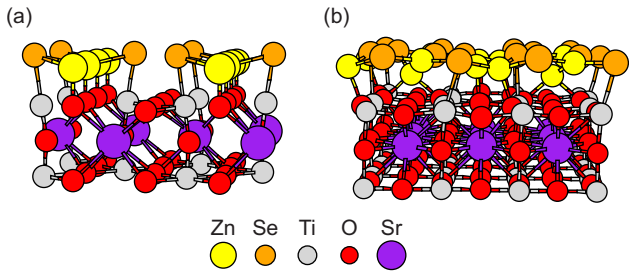

FIG. 3. (Color online) Perspective view of the lowest-energy (a) ZnSe(001)/STO(001) and (b) ZnSe(111)/STO(001) interfaces, as obtained starting from the assumed structures shown in Fig. 2.

structed along the same lines as described above. For the substrate, we adopt a (2×2) planar unit cell. This is the smallest unit cell consistent with polar-compensated configurations, which imply removing 1/4 of Zn atoms at the interface and accommodating them on the surface of the ZnSe(111) overlayer. Obviously, the hexagonal structure of the ZnSe(111) layers is not commensurate with the square lattice of STO(001). It can be matched at the expense of deforming the overlayer by +12.5% along $[11\bar{2}]_{\mathrm{ZnSe}}$ and −2.6% along $[1\bar{1}0]_{\mathrm{ZnSe}}$ (taking thermal coefficients into account does not affect these values), as sketched in Fig. 2(b). The hexagonal ZnSe(111) layer under such a strain becomes orthorhombic. After structural optimization, the most stable configuration shows highly distorted almost flat Se-Zn hexagonal rings, with Zn atop of O and Se atop of Ti [Fig. 3(b)]. Those rings, which run along $[100]_{\mathrm{STO}}$, are connected within each other through fourfold coordinated Zn atoms, which bind to two surface O and two Se atoms. The morphology of the (111) epilayer is akin to that of strained ZnSe(111) planes in the bulk crystal. The ZnSe overlayer appears to be internally well bound, as shown by the larger number of Zn-Se bonds than in the case of the ZnSe(001) single layer. Consistently, the formation energy of the ZnSe(111) overlayer is 7.18 eV/ZnSe unit, thus slightly larger with respect to ZnSe(001)/STO(001).[20]

IV. DISCUSSION

According to the computed formation energies, the HoC epitaxy is favored with respect to the CoC epitaxy, whenever two complete atomic Zn and Se planes are deposited on the $SrTiO_3$ surface and thermodynamic equilibrium is attained. The calculated difference $E_{\mathrm{form}}^{\mathrm{ZnSe}}(111)-E_{\mathrm{form}}^{\mathrm{ZnSe}}(001)=0.05$ eV/ZnSe, although small, represents a lower bound for the relative stability of the HoC epitaxy over the CoC epitaxy. Indeed, the ZnSe(111) single layer is very much strained as a consequence of the choice of the small (2×2) unit cell, as it can be seen by looking at the deformed hexagonal Zn-Se rings in Fig. 2(b). This is consistent with the evolution of the lattice parameter measured by RHEED [Fig. 1(c)], which indicates the existence of strained layers at the onset of growth. The emulation of a realistic coincidence cell with varying epilayer thickness would imply consideration of thousands of atoms, which is presently out of reach of *ab initio* methods. By adopting larger unit cells, several other possible configurations would be allowed, apart from the one that was actually computed for the (2×2) cell; therefore, the formation energy $E_{\mathrm{form}}^{\mathrm{ZnSe}}(111)$ would increase.

Consistently with the evolution of the lattice parameter of the ZnSe epilayer, the highly strained $ZnSe(111)/SrTiO_3(001)$ (2×2) configuration is not suited to represent realistic thicker overlayers. Within the elastic limit, the elastic energy of ZnSe(111) epilayers that corresponds to +12.5% strain along $[11\bar{2}]_{\mathrm{ZnSe}}$ and −2.6% strain along $[1\bar{1}0]_{\mathrm{ZnSe}}$ can be evaluated at 0.16 eV per ZnSe bulk unit cell.[21] On the contrary, the computed elastic energy corresponding to the CoC epitaxy amounts to less than 0.01 eV/ZnSe unit cell.

The difference of the elastic contributions between the HoC and CoC epitaxies is therefore $\Delta E_{\mathrm{elastic}}\simeq0.15$ eV/ZnSe unit. Beyond a threshold number of epilayers n_{crit}, the elastic contribution to the internal energy would unavoidably disfavor the HoC configuration with respect to the CoC one. Therefore, the computed $\Delta E_{\mathrm{form}}(n)=E_{\mathrm{form}}^{\mathrm{Zn}_n\mathrm{Se}_n}(111)-E_{\mathrm{form}}^{\mathrm{Zn}_n\mathrm{Se}_n}(001)$ between the HoC and CoC epitaxies is very much biased and not representative of the experimental situation whenever $n\geq n_{\mathrm{crit}}$. Within the constraints of the present $ZnSe(111)/SrTiO_3(001)$ (2×2) model, we find that $n_{\mathrm{crit}}\simeq2$. Note in Table I that $\Delta E_{\mathrm{form}}(2)=-0.12$ eV/ZnSe unit, which is almost equal to $-\Delta E_{\mathrm{elastic}}$.

Even in the absence of detailed simulations of thick ZnSe overlayers $(n\geq n_{\mathrm{crit}})$, we infer that the adhesion of the very first ZnSe plane drives the following growth. The (111)-oriented ZnSe single overlayer is more stable and shows larger internal cohesion than its (001) counterpart. The HoC growth of the first overlayer is thus governed by energetics, which is fully coherent with our observation that varying the growth temperature in the 180–280 °C range has no impact on the orientation of the ultrathin ZnSe layer. Once formed, the single ZnSe(111) overlayer on $SrTiO_3(001)$ can thus steer the growth of ZnSe along [111]. Indeed, its morphology is well suited for further growth of ZnSe(111), which is not the case of the chainlike first ZnSe(001) overlayer. Within our model the growth is no more driven by thermodynamics, and kinetics surely plays a role when $n\geq n_{\mathrm{crit}}$. After a 2D growth stage, with relaxation of the lattice parameter of the thicker ZnSe(111) overlayers, RHEED patterns show an increasing 3D character and indicate that kinetic roughening, associated with disorder, stacking faults [observed in TEM, Fig. 1(e)], and rotational domains, occurs.

Given the higher density of (111) planes than (001) ones in ZB structures, we think that the HoC growth is a prototypical case for the heteroepitaxy of several SC on cubic oxides, in presence of a large misfit. After GaAs,[6] InP,[7] and ZnSe, the next challenge is to investigate the growth of other chemically related ZB-SC on $SrTiO_3(001)$.

ACKNOWLEDGMENTS

We acknowledge support from D. Demaille, M. Selmane, and Y. Zheng for x-ray diffraction and TEM measurements. We thank C. Noguera for fruitful discussions. The computer resources used in this work were provided by IDRIS, CNRS, Orsay, France.

[1] E. Dagotto, Rev. Mod. Phys. **66**, 763 (1994).
[2] J. M. D. Coey, M. Viret, and S. von Molnar, Adv. Phys. **48**, 167 (1999).
[3] M. Imada, A. Fujimori, and Y. Tokura, Rev. Mod. Phys. **70**, 1039 (1998).
[4] D. P. Norton, Mater. Sci. Eng., R. **43**, 139 (2004).
[5] Y. Liang, J. Kulik, T. C. Eschrich, R. Droopad, Z. Yu, and P. Maniar, Appl. Phys. Lett. **85**, 1217 (2004).
[6] H. Fujioka, J. Ohta, H. Katada, T. Ikeda, Y. Noguchi, and M. Oshima, J. Cryst. Growth **229**, 137 (2001).
[7] G. Saint-Girons, C. Priester, P. Regreny, G. Patriarche, L. Largeau, V. Favre-Nicolin, G. Xu, Y. Robach, M. Gendry, and G. Hollinger, Appl. Phys. Lett. **92**, 241907 (2008).
[8] K. Nishida, Y. Kitamura, Y. Hijikata, H. Yaguchi, and S. Yoshida, Phys. Status Solidi B **241**, 2839 (2004).
[9] L. Carbonell, V. H. Etgens, A. Koëbel, M. Eddrief, and B. Capelle, J. Cryst. Growth **201-202**, 502 (1999), and references therein.
[10] Attempting the growth on vicinal substrates would, in this context, be an interesting way to reduce the variety of domains—a strategy which was successfully adopted in the case of CdTe (111)/GaAs (001), see A. Bourret, P. Fuoss, G. Feuillet, and S. Tatarenko, Phys. Rev. Lett. **70**, 311 (1993); J. Cibert, Y. Gobil, K. Saminadayar, S. Tatarenko, A. Chami, G. Feuillet, Le Si Dang, and E. Ligeon, Appl. Phys. Lett. **54**, 828 (1989).
[11] The full set of relationships is: $(111)_{ZnSe} \| (001)_{STO}$, and $[1\bar{1}0]_{ZnSe} \| [100]_{STO}$, $[1\bar{1}0]_{ZnSe} \| [010]_{STO}$, $[\bar{1}10]_{ZnSe} \| [100]_{STO}$, or $[\bar{1}10]_{ZnSe} \| [010]_{STO}$.
[12] G. Kresse and J. Hafner, Phys. Rev. B **47**, 558 (1993); G. Kresse and J. Furthmüller, Comput. Mater. Sci. **6**, 15 (1996); Phys. Rev. B **54**, 11169 (1996).
[13] P. E. Blöchl, Phys. Rev. B **50**, 17953 (1994).
[14] G. Kresse and D. Joubert, Phys. Rev. B **59**, 1758 (1999).
[15] H. J. Monkhorst and J. D. Pack, Phys. Rev. B **13**, 5188 (1976).
[16] J. Goniakowski, F. Finocchi, and C. Noguera, Rep. Prog. Phys. **71**, 016501 (2008).
[17] W. A. Harrison, E. A. Kraut, J. R. Waldrop, and R. W. Grant, Phys. Rev. B **18**, 4402 (1978).
[18] C. Noguera and J. Goniakowski, J. Phys.: Condens. Matter **20**, 264003 (2008).
[19] F. Bottin and F. Finocchi, Phys. Rev. B **76**, 165427 (2007).
[20] The most stable computed configurations found for the (001) or (111) ZnSe epitaxy are both semiconducting.
[21] R. A. Mayanovic, R. J. Sladek, and U. Debska, Phys. Rev. B **38**, 1311 (1988).